JOURNAL OF COLLOID AND INTERFACE SCIENCE **181,** 627–634 (1996)
ARTICLE NO. 0420

Adsorption Characteristics of Iron–Cyanide Complex on γ-Al_2O_3

W. P. CHENG AND CHIHPIN HUANG[1]

Institute of Environmental Engineering, National Chiao Tung University, Hsinchu, Taiwan, Republic of China

Received December 6, 1995; accepted February 26, 1996

The adsorption behavior of ferrocyanide and ferricyanide toward aluminum oxide with a 0.01 *M* $NaClO_4$ background electrolyte at 25°C was investigated. Results obtained from different pH values demonstrated that the adsorption of these complex ions could be described by a modified Langmuir isotherm in the concentration range 0.5×10^{-4} to 4×10^{-4} *M*. This modified Langmuir isotherm developed here could accurately predict the equilibrium partition between solid and liquid phases while taking proton competition into account. Also, the apparent equilibrium constant (K^{app}) derived from the Langmuir equation for ferrocyanide or ferricyanide adsorption on aluminum oxide was compared with the intrinsic constant (K^{int}) calculated by triple-layer model simulation. This comparison revealed a strong correlation between the apparent equilibrium constant and the intrinsic constant. Moreover, in comparing K^{app} with K^{int}, we can infer that the adsorption of either ferrocyanide or ferricyanide complexes onto aluminum oxide is achieved through outer-sphere complexation.

Key Words: **Langmuir model; triple-layer model; ferrocyanide; ferricyanide.**

INTRODUCTION

Adsorption phenomena involving inorganic ions and organic acids on hydrous oxides of aluminum, iron, manganese, and silica have been studied for the past three decades. More specifically, related topics including the effects of pH (1, 2), structural identity (3, 4), ionic strength (5–7), temperature effect (8, 9), and the nature of the adsorbent (10, 11) on the free ion adsorption have been extensively investigated. However, complex ion adsorption has received only limited attention.

Cyanide released from the industrial sector forms complexes with metal ions, e.g., iron, zinc, and nickel. Complexations readily occur since cyanide ions acting as strong ligands bind with metal ions to form metal–cyano complexes, thereby altering their original stability and toxicity. Although some metal–cyanide complexes, i.e., ferrocyanide $[Fe(CN)_6^{4-}]$ and ferricyanide $[Fe(CN)_6^{3-}]$, are less toxic than cyanide, they are not thermodynamically stable due to their slow decomposition kinetics under general soil conditions (12). When these complexes are exposed to light, free cyanide is released from the molecules by light irradiation (13). Therefore, in this study, two complex ions, ferrocyanide and ferricyanide, have been investigated with respect to their adsorption on the γ-Al_2O_3/water interface.

For the oxide/solution interface, the surface charge and potential gradient decrease with increasing distance from the interface to the solution phase. The concept of solution coordination chemistry is generally applied in describing adsorption of ions at the oxide/solution interface. The triple-layer model (TLM) developed by Hayes and Leckie (14) allows metal ions and anions to form an innersphere complexation at the surface layer (o-plane) or an outer-sphere complexation at the compact layer (β-plane) (15–17). This model also allows counterions to accumulate in a diffuse layer (d-plane) and a compact layer (β-plane). Consequently, a program, HYDRAQL (18), was developed to correlate the adsorption data with the triple-layer model concepts.

In addition to the TLM approach, a modified Langmuir model is developed here to describe the adsorption characteristics of ferrocyanide and ferricyanide onto γ-Al_2O_3 while taking proton competition into account. Based on theoretical assumptions, the apparent adsorption constant in the Langmuir model and the intrinsic surface complex constant in the TLM approach are differentiated by an electrostatic charge factor $[\exp(\Psi F/RT)]$. Kanungo (19) has suggested that the intrinsic constants are correctly estimated, if by comparing constants from the Langmuir isotherm and TLM, it can be determined whether inner-sphere or outer-sphere complexation occurs during the interaction between the ions and the oxide surface. The intrinsic constant seems to be higher than the apparent adsorption constant by an electrostatic term of the potential if the overall adsorption reaction is mostly contributed by the inner-sphere complexation. Actually, the competition of anions and cations with oxides for H^+ or OH^- ions allows the apparent adsorption constant in the Langmuir model to alter with the pH value. Therefore, the apparent adsorption constant in the Langmuir model is only available for comparison with the intrinsic constant in the surface complex model under low adsorption coverage and acidic conditions (20, 21).

[1] To whom correspondence should be addressed.

0021-9797/96 $18.00

Ferricyanide fails to bind with H^+, even at pH 1; however, ferrocyanide can bind with H^+, with two acidic constants, $pK_{a1} = 2.2$ and $pK_{a2} = 4.1$ (22). Hence, this study describes the differences in adsorption behavior of γ-Al_2O_3 for those complexes which possess equivalent stereostructure but nonequivalent proton-binding capacity. The apparent adsorption constant, derived from the modified Langmuir equation, can be provided as a parameter for TLM simulation by HYDRAQL. Simulation results show whether inner-sphere or outer-sphere complexation is the major type for ferricyanide or ferrocyanide adsorption onto γ-Al_2O_3. This study attempts to (a) investigate the proton effect on the adsorption of ferrocyanide and ferricyanide by the aluminum oxide–water interface, (b) derive a thermodynamic equilibrium constant from the Langmuir model while taking proton competition into account and then compare it with the intrinsic constant in TLM, and (c) determine the probable type of interaction between complexes and the oxide interface.

EXPERIMENTAL

Materials

Aluminum oxide (γ-Al_2O_3) (purity 99.6%; supplied by Japan Aerosol Co.) was used in this study. The oxide size produced was smaller than 1 μm and apparently uniform. Aluminum oxide was pretreated to increase its purity using the procedure suggested by Hohl and Stumm (23): 0.1 *N* NaOH was used to dissolve impurities on the oxide (i.e., SiO_2), followed by washing the oxide with distilled water several times to remove excess salts. Finally, the solid was dried overnight in an oven at 103°C. Stock solutions of $K_4Fe(CN)_6$ and $K_3Fe(CN)_6$ from the Riedel de Haen were prepared without further purification.

Batch Adsorption

Batch adsorption experiments were performed by transferring the aluminum oxide into 125-ml polyethylene bottles containing appropriate amounts of $NaClO_4$ and Milli-Q distilled water to yield the desired solid concentration and an ionic strength of 1×10^{-2} *M*. During the first 1 h, pH adjustments were made with HNO_3 or NaOH and the solids were shaken during this time. After 1 h, a given amount of $K_4Fe(CN)_6$ or $K_3Fe(CN)_6$ was added and mixed with the suspension and the pH was readjusted. After pH adjustment to values from 3 to 10 (with HNO_3 or NaOH under nitrogen atmosphere), the samples were shaken over a reciprocating shaker for 24 h at 25°C. At the end of this time, the suspension pH was measured and the solid was separated by membrane filtration with a 0.45-μm filter. Filtered supernatant was analyzed for residual Fe(II) or Fe(III) by flame atomic absorption spectroscopy on a Shimadzu 680 spectrophotometer. To investigate the possible release of free cyanide during adsorption, the concentration of free cyanide in the filtered supernatant was analyzed via polarography (Metrohm Model 693) using the method of differential pulse voltammetry. The half-wave potential for cyanide was -0.24 V in the 0.1 *M* KOH solution. It was found that CN^- was absent in the solution. Next, the effects of surface loading on adsorption were investigated by varying the initial iron–cyanide complex concentrations between 5×10^{-5} and 4×10^{-4} *M*, while all other conditions were kept constant.

MODEL DEVELOPMENT

The sites of oxide surface with the protolysis reactions of the hydroxyl group may be simulated as a surface ionization model (24). Electrolytes in a solution can form ion pairs with protonated or deprotonated hydroxyl groups on the surface. The triple-layer model follows that developed by Hayes and colleagues (14), in which the amphoteric ionization reaction on the surface of γ-aluminum oxide can be described as

$$AlOH_2^+ \rightleftharpoons AlOH + H^+$$

$$K_{a1}^{int} = \frac{[AlOH][H^+]}{[AlOH_2^+]} \exp\left(\frac{-\Psi_0 F}{RT}\right)$$

and

$$AlOH \rightleftharpoons AlO^{-1} + H^+$$

$$K_{a2}^{int} = \frac{[AlO^-][H^+]}{[AlOH]} \exp\left(\frac{-\Psi_0 F}{RT}\right),$$

where R is the gas constant, F is the Faraday constant, and K_{a1}^{int} and K_{a2}^{int} are considered the first and second intrinsic acidity constants of the γ-Al_2O_3 surface. To account for the adsorption of the counterion, Yates *et al.* (25) proposed that nonspecific ion pair adsorption occurs at the charged sites as described below,

$$AlOH + Na^+ \rightleftharpoons AlO^- - Na^+ + H^+$$

$$K_{Na+}^{int} = \frac{[AlO^- - Na^+][H^+]}{[AlOH][Na^+]} \exp\left\{\frac{(\Psi_\beta - \Psi_o)F}{RT}\right\}$$

$$AlOH + H^+ + ClO_4^- \rightleftharpoons AlOH^+ - ClO_4^-$$

$$K_{ClO4-}^{int} = \frac{[AlOH^+ - ClO_4^-]}{[AlOH][ClO_4^-][H^+]} \exp\left\{\frac{(\Psi_0 - \Psi_\beta)F}{RT}\right\},$$

where Ψ_0 and Ψ_β are the o-plant and β-plane electrostatic potential (V), respectively, and K_{Na+}^{int} and K_{ClO4-}^{int} are the surface complexation constants of background electrolytes Na^+ and ClO_4^-, respectively.

Two types of chemical bonding, i.e., coordination (located at the o-plane) and ion pair (located at the β-plane), are initially assumed in the HYDRAQL simulation. This simula-

TABLE 1
Parameters of the Triple-Layer Model for γ-Al_2O_3

Specific surface areas (m^2/g)	118
Site density (site/nm^2)	1.3
Capacitance C_1, C_2 (μF/cm^2)	140, 20
log K_{a1}^{int} log K_{a2}^{int}	7.2, 9.5
log K_{Na+}^{int} log K_{ClO4-}^{int}	9.1, 8.2

tion for adsorption edges at different pH values for various ferrocyanide or ferricyanide concentrations includes known values of C_1, C_2, N_t, K_{a1}^{int}, K_{a2}^{int}, K_{Na+}^{int}, and K_{ClO4-}^{int}. The surface acidity and surface complex constants used in the modeling are $pK_{a1}^{int} = 7.2$, $pK_{a2}^{int} = 9.5$, and $pK_{Na+}^{int} = 9.1$ as previously determined by Hohl and Stumm (23); pK_{ClO4-}^{int} is assumed to be equivalent to pK_{Cl-}^{int} (=8.2). The value of N_t for oxide must first be specified in the HYDRAQL program and is determined according to

$$N_t = \frac{C * A_{sp} * N_s}{N} \times 10^{18} \text{ (mol/liter)},$$

where

C = concentration of aluminum oxide solid (g/liter)
A_{sp} = specific surface area (m^2/g)
N_s = site density (site/nm^2)
N = Avogadro's number (6.02×10^{23}/mol).

The specific surface are of aluminum oxide (A_{sp}) as measured by the BET method was 118 m^2/g, which is similar to the results of Hohl and Stumm (23). Also, their recorded side density was 1.3 OH groups/nm^2. For the capacitance of C_1 and C_2, Zhang *et al.* (26) found that the optimum correlations for the acid–base titration data of Schulthess and Sparks (27) were $C_1 = 1.4$ μF/m^2 and $C_2 = 0.2$ μF/m^2. Table 1 gives the rule sheet for the triple-layer model.

RESULTS AND DISCUSSION

Modified Langmuir Isotherm

The simple Langmuir form is expected to hold for a clean, smooth, nonporous surface, showing reversible, physical adsorption of a pure solute. The aluminum oxide surface is an adsorbent capable of adapting to the conditions that the Langmuir theory expects. Ferrocyanide and ferricyanide possess high valence numbers. That is, a situation in which adsorption occurs uniformly over the aluminum oxide surface causes the colloid surface to be more negatively charged, and subsequently interferes with anion adsorption on the surface. Moreover, stable iron–cyanide complexes maintain their dissolved condition regardless of an increase in concentration. Therefore, the adsorption of an iron–cyanide complex on the surface can form only a monolayer coverage as assumed by the hypotheses of Langmuir isotherm. Thus, ferricyanide or ferrocyanide adsorption on aluminum oxide surfaces may be described by an individual step as

$$\text{AlOH} + m\text{H}^+ + \text{Fe(CN)}_6^{n-} \rightleftharpoons \text{AlOH}_2^+ - \text{H}_{m-1}\text{Fe(CN)}_6^{(n-m+1)-} \quad [1]$$

$$K^{app} = \frac{[\text{AlOH}_2^+ - \text{H}_{m-1}\text{Fe(CN)}_6^{(n-m+1)-}]}{[\text{AlOH}][\text{H}^+]^m[\text{Fe(CN)}_6^{n-}]}, \quad [2]$$

where n, equal to 3 and 4, represents ferricyanide and ferrocyanide, respectively, and K^{app} is the apparent adsorption constant. As previously mentioned, the ferrocyanide ($Fe(CN)_6^{4-}$) ion can form conjugate acids, i.e., $HFe(CN)_6^{3-}$. It has been also suggested that ferricyanide ($Fe(CN)_6^{3-}$) has no evidence for the formation of conjugate acid above pH 1 (22). Therefore, the m values in Eq. [1] for ferrocyanide and ferricyanide are defined as 2 and 1, respectively. In a simplified plot form, Kurbatov and colleagues (28) plotted $\log[\text{AlOH}_2^+ - \text{H}_{m-1}\text{Fe(CN)}_6^{(n-m+1)-}]/[\text{Fe(CN)}_6^{n-}]$ vs pH. The slope of this curve provides insight into m. However, the data must be interpreted carefully since m varies with pH and may vary with the adsorption coverage (29). For an exact analysis of the proton stoichiometry, Langmuir theory allows the m value to be an integral.

C_{SF}, C_S, and C_F are represent $[\text{AlOH}_2^+ - \text{H}_{m-1}\text{Fe(CN)}_6^{(n-m+1)-}]$, [AlOH], and $[\text{Fe(CN)}_6^{n-}]$, respectively. Also, C_T is equivalent to the combination of C_{SF} and C_F with a given molar concentration of the $Fe(CN)_6^{n-}$ solution. Equation [2] can then be rewritten as

$$C_{SF} = \frac{K^{app} C_S C_T [\text{H}^+]^m}{1 + K^{app} C_S [\text{H}^+]^m} \quad [3]$$

and

$$C_S = C_{Max} - C_{SF}, \quad [4]$$

in which C_{Max} represents the maximum value of C_{SF}. Combining Eqs. [3] and [4] yields

$$C_{SF} = \frac{K^{app} C_F C_{Max} [\text{H}^+]^m}{1 + K^{app} C_F [\text{H}^+]^m}. \quad [5]$$

By using a double-reciprocal plot (Langmuir plot), i.e., C_F/C_{SF} vs C_F, Eq. [5] can be rearranged as

$$\frac{C_F}{C_{SF}} = \frac{1}{K^{app} C_{Max} [\text{H}^+]^m} + \frac{1}{C_{Max}} C_F. \quad [6]$$

In this plot, C_{Max} and K^{app} can be obtained from the intercept and slope of the plot for fixed pH. Figures 1a and 1b

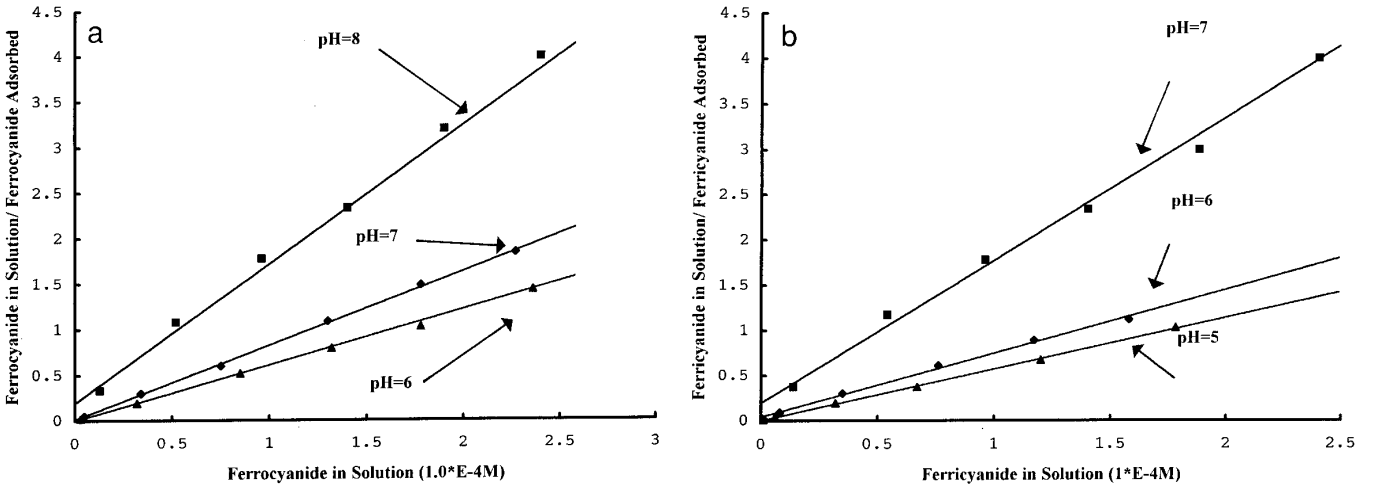

FIG. 1. Langmuir plots for (a) ferrocyanide and (b) ferricyanide adsorption isotherms on the γ-Al_2O_3 surface at three pH values.

illustrate the Langmuir plots for ferrocyanide and ferricyanide adsorption isotherms on the γ-Al_2O_3 surface at three pH values. The best fit of these plots has been conducted with linear regression to obtain C_{Max} and K^{app} values as listed in Table 2. The results indicate that adsorption capacity (C_{Max}) values range from a lowest value of 6.35×10^{-5} for ferricyanide at pH 8 to a highest value of 1.83×10^{-4} for ferrocyanide at pH 5. The table also indicates that C_{Max} decreases with pH, which may be explained by the evidence that surface protonation increases with a decrease in pH. This increase results in more positively charged sites on the surface, thereby enlarging the attraction force existing between aluminum oxide and adsorbate. This enlarging of the adsorption force has originated from a large valence number of ferrocyanide which can conjugate with the proton located at the interface through hydrogen bonding. Therefore, the adsorption capacity of ferrocyanide is higher than that of ferricyanide at the same pH as listed in Table 2.

TLM Modeling

Figures 2 and 3 summarize the effects of pH, ranging from 4 to 10, on the adsorption of ferrocyanide or ferricyanide with three different concentrations onto the aluminum oxide surface. Figures 2a and 2b represent the pH edges for ferricyanide adsorption fitted by the TLM simulation with outer-sphere complexation and inner-sphere complexation, respectively. Figures 3a and 3b are also the pH edges but for ferrocyanide adsorption fitted by TLM simulation with outer-sphere complexation and inner-sphere complexation, respectively. From these results, adsorption capacity percentages of ferrocyanide and ferricyanide anions decrease with increased pH.

According to the assumptions of the triple-layer model, cations or anions if present in the solution are allowed to form surface complexes at either the o-plane (inner-sphere complexation) or the β-plane (outer-sphere complexation). Surface reactions of ferrocyanide $[Fe(CN)_6^{4-}]$ or ferricyanide $[Fe(CN)_6^{3-}]$ on the β-plane may include

$$\text{AlOH} + \text{Fe(CN)}_6^{n-} + \text{H}^+ \rightleftharpoons \text{AlOH}^{2+} - \text{Fe(CN)}_6^{n-} \quad [7]$$

$$K_{\text{Fel}}^{\text{int}} = \frac{[\text{AlOH}^{2+} - \text{Fe(CN)}_6^{n-}]}{[\text{AlOH}][\text{Fe(CN)}_6^{n-}][\text{H}^+]} \exp\left\{\frac{[\Psi_0 - n\Psi_\beta]F}{RT}\right\} = K_{\text{Fel}}^{\text{app}} \exp\left\{\frac{[\Psi_0 - n\Psi_\beta]F}{RT}\right\}$$

$$\text{AlOH} + \text{Fe(CN)}_6^{n-} + 2\text{H}^+ \rightleftharpoons \text{AlOH}^{2+} - \text{HFe(CN)}_6^{(n-1)-} \quad [8]$$

$$K_{\text{Fe2}}^{\text{int}} = \frac{[\text{AlOH}^{2+} - \text{HFe(CN)}_6^{(n-1)-}]}{[\text{AlOH}][\text{Fe(CN)}_6^{n-}][\text{H}^+]^2} \times \exp\left\{\frac{[\Psi_0 - (n-1)\Psi_\beta]F}{RT}\right\} = K_{\text{Fel}}^{\text{app}} \exp\left\{\frac{[\Psi_0 - (n-1)\Psi_\beta]F}{RT}\right\}.$$

Surface reactions at the o-plane may include

$$\text{AlOH} + \text{Fe(CN)}_6^{n-} + \text{H}^+ \rightleftharpoons \text{AlFe(CN)}_6^{(n-1)-} + \text{H}_2\text{O} \quad [9]$$

$$K_{\text{Fe3}}^{\text{int}} = \frac{[\text{AlFe(CN)}_6^{(n-1)-}]}{[\text{AlOH}][\text{Fe(CN)}_6^{n-}][\text{H}^+]} \exp\left\{\frac{-(n-1)\Psi_0 F}{RT}\right\} = K_{\text{Fe3}}^{\text{app}} \exp\left\{\frac{-(n-1)\Psi_0 F}{RT}\right\}$$

TABLE 2

C_{Max} and K^{app} Values of the Langmuir Model for Ferrocyanide and Ferricyanide Adsorption at Three pH Values

Ferrocyanide			Ferricyanide		
pH	C_{Max} (mol/liter)	K (l mol^{-1})	pH	C_{Max} (mol/liter)	K (l mol^{-1})
6	1.67×10^{-4}	3.22×10^{18}	5	1.83×10^{-4}	7.22×10^{10}
7	1.23×10^{-4}	8.16×10^{19}	6	1.42×10^{-4}	1.81×10^{11}
8	6.35×10^{-5}	7.97×10^{20}	7	6.50×10^{-5}	6.38×10^{11}

$$\mathrm{AlOH} + \mathrm{Fe(CN)}_6^{n-} + 2\mathrm{H}^+ \rightleftharpoons \mathrm{AlHFe(CN)}_6^{(n-2)-} + \mathrm{H_2O} \quad [10]$$

$$K_{\mathrm{Fe4}}^{\mathrm{int}} = \frac{[\mathrm{AlHFe(CN)}_6^{(n-2)-}]}{[\mathrm{AlOH}][\mathrm{Fe(CN)}_6^{n-}][\mathrm{H}^+]^2} \exp\left\{\frac{-(n-2)\Psi_0 F}{RT}\right\} = K_{\mathrm{Fe4}}^{\mathrm{app}} \exp\left\{\frac{-(n-2)\Psi_0 F}{RT}\right\}.$$

Several studies have suggested that the equivalent Langmuir adsorption constant (K^{app}) is typically different in a large order from the surface complex formation equilibrium constant (K^{int}) (30, 31). Stumm (32) has indicated that K^{int} can be converted into K^{app}. Therefore, in this study, the average equilibrium constants calculated from the result of Table 2 ($K^{app} = 10^{11.3}$ for ferricyanide and $10^{19.8}$ for ferrocyanide) were used as K^{int} in Eqs. [7]–[10] of the triple-layer model. Owing to the failure of proton binding, ferricyanide adsorption at the interface requires Eqs. [7] and [9] to represent only outer-sphere and inner-sphere complexation. According to the pK_{a2} of ferrocyanide (=4.1), a more acidic environment occurs at the interface than in the bulk. Hence, pH_s (pH at the interface) is different from pH measured in the bulk (pH_b). That relationship can be expressed as

$$\mathrm{pH_s} = \mathrm{pH_b} + \frac{e\Psi}{2.3kT},$$

where k is Boltzmann's constant. At a typical Ψ value of 200 mV, a difference of 3–4 pH units between pH_s and pH_b is possible (33). Therefore, Eqs. [8] and [10], involving a proton conjugated with the ferrocyanide complex, are two reasonable equations for expressing outer-sphere and inner-sphere complexations.

As known, K^{app} and K^{int} are differentiated by an electrostatic charge factor (=$\exp(\Psi F/RT)$). A comparison of the intrinsic constant and the apparent constant provides further insight into understanding whether inner-sphere or outer-sphere complexation occurs in the adsorption. The K_{a1}^{int} and K_{a2}^{int} of γ-Al_2O_3 are 7.2 and 9.5, respectively, as listed in Table 1. The calculated pH_{pzc} of γ-Al_2O_3 by taking the average of pK_{a1}^{int} and pK_{a2}^{int} is 8.35. Because anion adsorption can result in a decrease in pH_{pzc} (34), pH_{pzc} can possibly drop into the pH range (i.e., 6 ~ 8) of the iron–cyanide adsorption experiment. Therefore, such an operational pH similar to pH_{pzc} causes a small electrostatic charge factor and K^{app} can be assumed to be close to K^{int}. As a result, an average of K^{app} in Table 2 provides a substitutive parameter for K^{int} in the TLM simulation with HYDRAQL.

Figures 2a and 2b display the TLM results simulated by using two types of surface complexation as suggested in Eqs. [7] and [9]. The solid lines shown in Fig. 2a were obtained by applying HYDRAQL under the assumption of the outer-sphere complexation (Eq. [7]). Figure 2a reveals

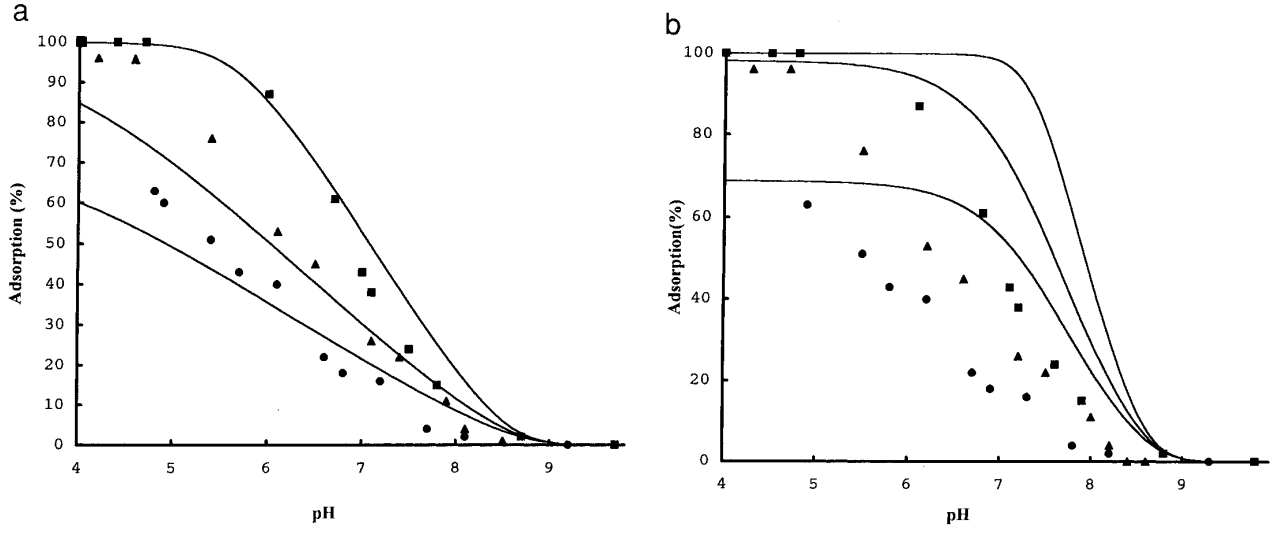

FIG. 2. HYDRAQL simulation of adsorption edges of ferricyanide as a function of pH with log K^{int} = 11.3: (a) outer-sphere and (b) inner-sphere complexation. Initial ferricyanide concentrations: (■) 1×10^{-4} *M;* (▲) 2×10^{-4} *M;* and (●) 3×10^{-4} *M.*

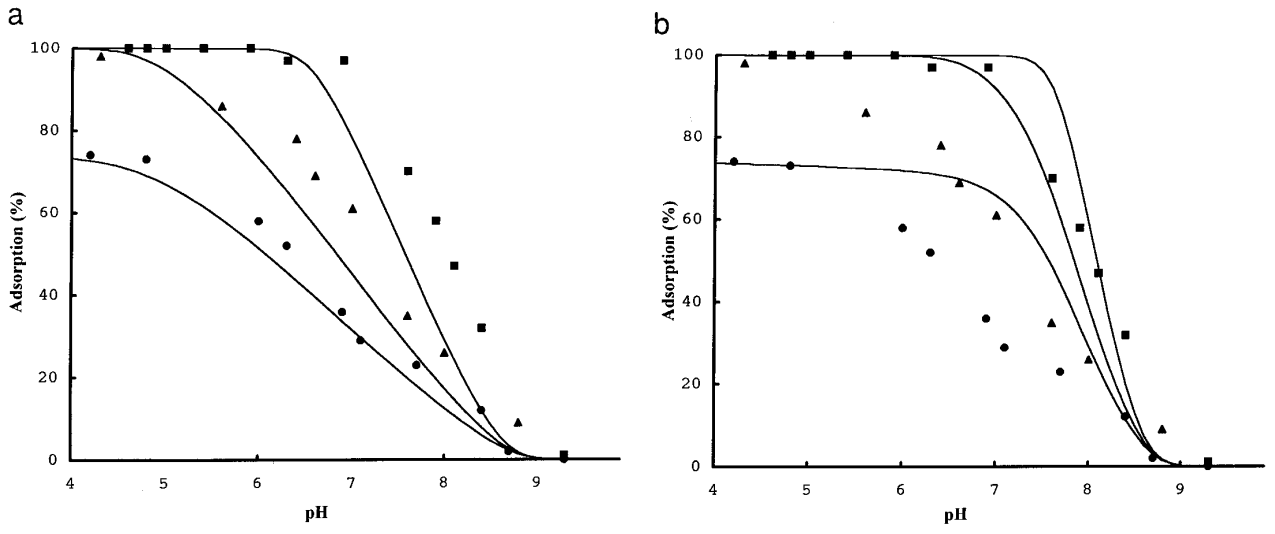

FIG. 3. HYDRAQL simulation of adsorption edges of ferrocyanide as a function of pH with log K^{int} = 19.8: (a) outer-sphere and (b) inner-sphere complexation. Initial ferrocyanide concentrations: (■) 1×10^{-4} *M;* (▲) 2×10^{-4} *M;* and (●) 3×10^{-4} *M.*

a sufficient correlation of simulation results with the experimental data. In contrast, under the assumption of inner-sphere complexation as in Eq. [9], the simulation results of the adsorption percentage are higher than the experimental results (Fig. 2b). According to the formulus of K^{int} in Eq. [9], a smaller assumption for K^{int} may obtain a better corresponding result. However, attaining a K^{int} lower than K^{app} is impossible, since, under the assumption of inner-sphere complexation of ferricyanide, a negative potential occurs on the o-plane, which indicates a positive electrostatic charge factor. The positive factor represents a K^{int} larger than K^{app}, thereby implying an impossible occurrence of inner-sphere complexation. Therefore, the mechanism of ferricyanide adsorption on the γ-aluminum oxide surface is obviously contributed by the outer-sphere complexation.

Figures 3a and 3b illustrate the pH-edge results of ferrocyanide adsorption. The data were also correlated by applying HYDRAQL under the assumption of outer-sphere complexation (Eq. [8]) and inner-sphere complexation (Eq. [10]). Figure 3a confirms a sufficient correlation between simulated and experimental results. As with ferricyanide, an average apparent constant of ferrocyanide ($K^{app} = 6.31 \times 10^{19}$, see Table 2), used as a substitute for the intrinsic constant (K^{int}) in HYDRAQL with the assumption of outer-sphere complexation as described in Eq. [8], can accurately describe experimental data. From the above considerations, we can conclude that the adsorption of the ferrocyanide ion on the γ-Al_2O_3 surface is an outer-sphere reaction. Figures 4a and 4b summarize the simulation results on model prediction by increasing the intrinsic constant from 6.31×10^{19} to 1.26×10^{21}. These figures suggest that the TLM provides a reasonably good prediction of K^{int} at 1.26×10^{21}. The results also demonstrate that the value of $\Psi_0 - 3\Psi_\beta$ can be determined by $\ln K^{int} - \ln K^{app}$. The $\Psi_0 - 3\Psi_\beta$ value is 0.0768 V, which is in the range of results listed in Table 3.

As indicated in the previous section by both the fitting results indicated and the discussion regarding electrostatic charge factor, outer-sphere complexation is clearly the only adsorption behavior for either ferricyanide or ferrocyanide on the oxide. The experimental values of the apparent equilibrium constant (K^{app}) at various pH values can be facultative in distinguishing between inner- and outer-sphere complexes. Table 2 indicates that K^{app} increases with pH. However, the value of K^{int} is independent of pH from a theoretical perspective. Therefore, the values of ($\ln K^{int} - \ln K^{app}$) decrease as pH increases, thereby implying that the value of ($\Psi_0 - 3\Psi_\beta$) decreases as pH increases. This occurrence can be verified with respect to the results as indicated in Table 3. That is, under data simulated by HYDRAQL, the surface potential decreases as pH increases for three concentrations of iron–cyanide.

Table 2 also reveals only a slight pH effect on the K^{app} for the ferricyanide adsorption. However, the Langmuir model fails to account for the change in the extent of adsorption which occurs when the aqueous phase composition is altered in pH. However, the extent of ion adsorption is markedly affected by pH. This effect is attributed to the fact that both the surface acidity and the hydrolysis of the ions are pH-dependent. Therefore, changing the pH values may also alter the number of positive charge sites of metal oxide and complex ions. A comparison of TLM and the Langmuir model reveals that the major advantage of the TLM is its consideration of the proton effect for adsorbent, adsorbate, and surface charge effect. Therefore, the apparent equilibrium constant calculated with the Langmuir model simulation is theoretically quite different from the intrinsic constant

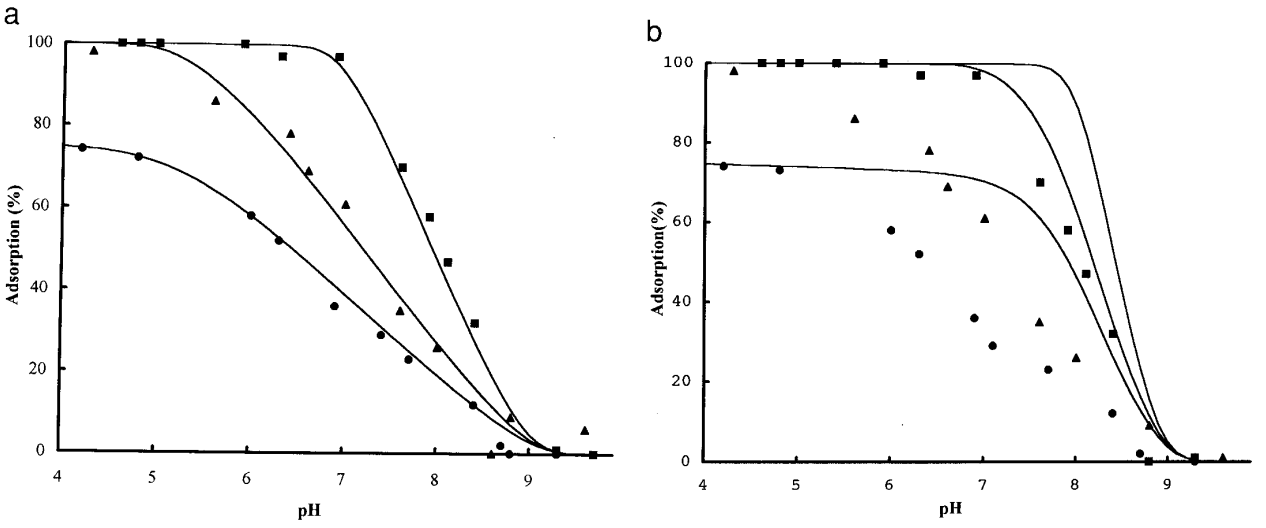

FIG. 4. HYDRAQL simulation of adsorption edges of ferrocyanide as a function of pH with log K^{int} = 21.1: (a) outer-sphere and (b) inner-sphere complexation. Initial ferrocyanide concentrations: (■) 1×10^{-4} *M;* (▲) 2×10^{-4} *M;* and (●) 3×10^{-4} *M.*

determined by TLM simulation. However, in this study, a close correction between apparent equilibrium constants (Table 2) and the intrinsic constant for either ferrocyanide or ferricyanide adsorption on the aluminum oxide surface is obtained. This result may be accounted for by the following reasons: (a) The modified Langmuir equation used in Eq. [1] includes the proton in the overall reaction. (b) When the acidic conjugation constant is considered, ferricyanide is still stable with H^+ ions even at pH lower than 1. Therefore, the *m* value in Eq. [1] or [2] is independent of pH and can be defined as 1. It is a particular phenomenon not having occurred on an anion. Conversely, ferrocyanide with a pK_{a2} of 4.2 has a high likelihood of causing competition of protons at the interface with the oxide. Hence, the pH effect on the *m* value for the ferrocyanide is more significant than that for the ferricyanide, thereby resulting in a more significant pH effect on K^{app} for ferrocyanide. This assumption can be verified according to the results in Table 2 and can also provide a reasonable explanation for the better correlation in Fig. 2a than in Fig. 3a. (c) As already mentioned, the apparent equilibrium constant is almost equivalent to the intrinsic constant if the solution pH value is near the pH_{pzc} of aluminum oxide. More specifically, anion adsorption by the oxide can result in a significant decrease of pH_{pzc}. In this study, the pH_{pzc} is dropped from 8.35 to lower pH values during the adsorption of iron–cyanide. Therefore, the resulting pH_{pzc} was in the range of the experimental pH, thereby resulting in a close correlation between the apparent equilibrium constant and the intrinsic constant (35).

TABLE 3
Surface Potential of Aluminum Oxide in the Presence of Ferricyanide or Ferrocyanide Adsorption[a]

Initial concentration	pH	Ψ_0	Ψ_β	$\Psi_0 - 3\Psi_\beta$
Ferricyanide				
1×10^{-4} *M*	5	0.138	0.0328	0.0396
	6	0.090	0.0096	0.0611
	7	0.048	−0.00147	0.0522
2×10^{-4} *M*	5	0.1220	−0.0031	0.1313
	6	0.0833	−0.0075	0.1057
	7	0.0444	−0.0107	0.0765
3×10^{-4} *M*	5	0.1180	−0.0112	0.1516
	6	0.0427	−0.0133	0.1210
	7	0.0427	−0.0152	0.0883
Ferrocyanide				
1×10^{-4} *M*	6	0.0853	−0.0022	0.0919
	7	0.0388	−0.0253	0.1147
	8	0.006	−0.0175	0.0585
2×10^{-4} *M*	6	0.0661	−0.0522	0.2227
	7	0.0338	−0.0388	0.1502
	8	0.0033	−0.0241	0.0756
3×10^{-4} *M*	6	0.0628	−0.0608	0.2452
	7	0.0320	−0.0441	0.1643
	8	0.0018	−0.0277	0.0849

[a] Potential unit, volt.

CONCLUSION

The results in this study have demonstrated that the concentrations of protonated surface hydroxyls and adsorption capacities of ferrocyanide and ferricyanide decrease as pH increases. A modified Langmuir isotherm developed here could accurately predict the equilibrium partition between solid and liquid phases at adsorbate concentrations lower than 4×10^{-4} *M.* The apparent equilibrium constants increase with pH, thereby implying that the values of the elec-

trostatic charge factor ($\Psi_0 - 3\Psi_\beta$) decrease as pH increases. While considering the acidic conjugation constant, ferricyanide remains stable with H^+ ions even at a pH lower than 1, thereby resulting in a significantly lower pH effect on the K^{app} for the ferricyanide. On the contrary, the natural promotion in adsorption capacities of ferrocyanide is attributed primarily to the stronger lateral interactions exerted for ferrocyanide conjugated with H^+ at the γ-aluminum oxide surface to form hydrogen bonding.

Under the assumption of outer-sphere complexation, the triple-layer model, with the Langmuir adsorption constant substituted for the surface complex formation equilibrium constant, can closely simulate the pH edge of ferrocyanide and ferricyanide adsorption by γ-aluminum oxide. The Langmuir adsorption constant is found to be of the same order as the surface complex formation equilibrium constant.

REFERENCES

1. Bar-Yosef, B., 1979., *Soil Sci. Soc. Am. J.* **43,** 1095 (1979).
2. Kinniburgh, D. G., and Jackson, M. L., *Soil Sci. Soc. Am. J.* **46,** 56 (1982).
3. Papelis, C., *Environ. Sci. Technol.* **29,** 1526 (1995).
4. Roe, L. A., Hayes, K. F., and Chisholm-Brause, C., *Langmuir* **7,** 367 (1991).
5. Mclaren, R. G., Swift, R. S., and Williams, J. G., *J. Soil Sci.* **32,** 247 (1981).
6. Swallow, K. C., Hume, D. N., and Morel, F. M. M., *Environ. Sci. Technol.* **14,** 1326 (1980).
7. Rodda, D. P., Johnson, B. B., and Wells, J. D., *J. Colloid Interface Sci.* **161,** 57 (1993).
8. Srivastava, A., and Srivastava, P. C., *Environ. Pollut.* **68,** 171 (1990).
9. Mehrian, T., de Keizer, A., and Lyklema, J., *Langmuir* **7,** 3094 (1991).
10. Bradley, S. M., Kydd, R. A., and Howe, R. F., *J. Colloid Interface Sci.* **159,** 405 (1993).
11. Kawakami, H., and Yoshida, S., *J. Chem. Soc. Faraday Trans. 2.* **81,** 1117 (1985).
12. Knowles, C. J., *Bacterial. Rev.* **40,** 652 (1976).
13. Meeussen, J. C. L., Keizer, M. G., and de Haan, F. A. M., *Environ. Sci. Technol.* **26,** 511 (1992).
14. Hayes, K. F., and Leckie, J. O., *J. Colloid Interface Sci.* **115,** 564 (1987).
15. Hayes, K. F., Papelis, C., and Leckie, J. O., *J. Colloid Interface Sci.* **125,** 717 (1988).
16. Hayes, K. F., Redden, G., Ela, W., and Leckie, J. O., *J. Colloid Interface Sci.* **142,** 448 (1991).
17. Katz, L. E., and Hayes, K. F., *J. Colloid Interface Sci.* **170,** 477 (1995).
18. Papelis, C., Hayes, K. F., and Leckie, J. O., ''HYDRAQL,'' Technical Report No 306. Stanford University.
19. Kanungo, S. B., *J. Colloid Interface Sci.* **162,** 93 (1994).
20. Benjamin, M. M., and Leckie, J. O., *J. Colloid Interface Sci.* **79,** 209 (1981).
21. Hazvey, D. T., and Fulghum, J. F., *J. Colloid Interface Sci.* **94,** 276 (1983).
22. Eaton, W. A., George, P., and Hanania, G. I. H., *J. Phys. Chem.* **71,** 2016 (1967).
23. Hohl, M., and Stumm, W., *J. Colloid Interface Sci.* **55,** 281 (1976).
24. Huang, C. P., and Stumm, W., *J. Colloid Interface Sci.* **43,** 409 (1973).
25. Yates, D. E., Levine, S., and Healy, T. E., *J. Chem. Soc. Faraday Trans. 1.* **70,** 1807 (1974).
26. Zhang, Z. Z., Sparks, D. L., and Scriver, N. C., *J. Colloid Interface Sci.* **162,** 244 (1994).
27. Schulthess, C. P., and Sparks, D. L., *Soil Sci. Soc. Am. J.* **50,** 1406 (1986).
28. Kurbatov, M. H., Wood, G. B., and Kurbatov, J. D., *J. Phys. Chem.* **55,** 1170 (1951).
29. Honeyman, B. O., and Leckie, J. O., *in* ''Geochemical Processes at Mineral Surface'' (J. A. Davis and Hayes, K. F., Eds.). ACS symposium, Washington, DC, 1986.
30. Hsia, T. H., Lo, S. L., and Lin, C. F., *Chemosphere* **25,** 1825 (1992).
31. Spanos, N., Slove, S., and Kordulis, Ch., *Langmuir* **10,** 3134 (1994).
32. Stumm, W., ''Chemistry of the Solid–Water Interface,'' p. 90. Wiley, New York, 1992.
33. Tewari, P. H., and Lee, W., *J. Colloid Interface Sci.* **52,** 77 (1975).
34. Stumm, W., and Morgan, J., ''Aquatic Chemistry,'' p. 633. Wiley, New York, 1981.
35. Johnson, R. E., *J. Colloid Interface Sci.* **100,** 540 (1984).